INSTITUTE OF PHYSICS PUBLISHING PLASMA PHYSICS AND CONTROLLED FUSION

Plasma Phys. Control. Fusion **47** (2005) A307–A315 doi:10.1088/0741-3335/47/5A/022

Wave stimulated phenomena in inductively coupled magnetized plasmas

K P Shamrai[1], S Shinohara[2], V F Virko[1], V M Slobodyan[1], Yu V Virko[1] and G S Kirichenko[1]

[1]Institute for Nuclear Research, National Academy of Sciences, Kiev 03680, Ukraine
[2]Interdisciplinary Graduate School of Engineering Sciences, Kyushu University, Kasuga, Fukuoka 816-8580, Japan

Received 29 October 2004
Published 20 April 2005
Online at stacks.iop.org/PPCF/47/A307

Abstract

Linear and nonlinear wave phenomena and their influence on the discharge performance are considered in the helicon plasma (HP) and magnetized inductively coupled plasma (MICP). Magnetic field configuration is shown to result in strong variation in the efficiency of plasma production caused by alterations of the character of wave processes rather than by the particle confinement. Effects of magnetic configuration are found to be dominant in operation of the compact HP with permanent magnet. Low frequency turbulence in the megahertz range is revealed to be inherent for both the HP and MICP and to depend strongly on the magnetic configuration. Enhanced axial electric field arising in front of the metal end plate in the HP is argued to be a potential source of the nonlinear effects.

1. Introduction

Inductively coupled magnetized plasmas (ICMPs) are advanced tools for producing dense, low-temperature plasmas over a broad range of parameters. These devices are known in two basic configurations. A helicon plasma (HP) uses a shell antenna that envelops the dielectric discharge chamber and launches the rf power across the magnetic field [1, 2]. A magnetized inductively coupled plasma (MICP) operates with a flat antenna depositing the power through a dielectric window along the magnetic field [3–5]. The variety of these sources has been developed for applications and basic research, such as materials surface processing, space propulsion, decomposition of hazardous substances, modelling of space phenomena, etc (e.g. [2, 6–10]) including the compact sources with permanent magnets (PMs) [11–14].

The operation of the ICMPs is governed by diverse linear and nonlinear processes stimulated by the waves that are excited directly, by the antenna, and indirectly, via inherent cooperative phenomena. By controlling these processes, one can increase the power absorption and improve plasma confinement, thus increasing the plasma output. Two methods reported

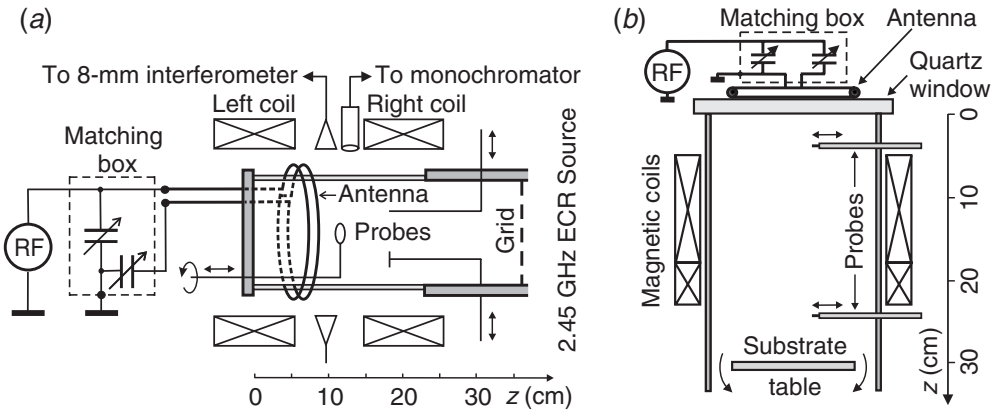

Figure 1. Schematic view of the large experimental devices: (*a*) the HP source and (*b*) the MICP source.

to enhance plasma production in the HPs are based on linear properties of the waves at the fundamental frequency. The first permits doubling of the plasma density with the use of helical or phased antennas and originates from directional plasma production along the $m = +1$ helicon mode propagation [15–17]. The second method results in multifold increase of the plasma output in a nonuniform (converging) magnetic field [18–20] and is thought to arise from peculiarities of the group velocity and mode conversion of the helicon waves [20]. The effect of nonuniform magnetic field has to be especially strong in the compact ICMPs with PMs.

Other potentialities for controlling the source are nonlinear and turbulent processes. Nonlinear effects stimulated by the rf field in non-magnetized ICPs (see [21] and references therein) can also work in the ICMPs. Many extra effects can be caused by the presence of the magnetic field and by the wave excitation; e.g. electron drift current driven [22] and parametric [23, 24] instabilities. Recent experiments with the HPs have revealed the excitation of turbulence in the megahertz frequency range [25–30] which can result in additional rf power absorption and particle heating [31, 32]. Turbulence excited by the drift instability in the range of tens of kilohertz is unwanted as it can worsen plasma confinement [33]. Ponderomotive force in the HP can have an influence on radial plasma stability [34]. Some nonlinear effects were also detected in the MICP, such as generation of the rf harmonics [35].

This paper briefly discusses some wave phenomena and argues their dominance over the discharge operation and potentiality to maximize the plasma output in the ICMPs with azimuthally symmetric ($m = 0$) antennas. In section 2, we describe the devices used in our investigations. The effect of magnetic field configuration on the operating regimes and the efficiency of plasma production is considered in section 3. In section 4, low-frequency turbulence in the large HP and MICP is characterized and the ponderomotive force predicted to arise near the metal end plate is analysed. In section 5, conclusions are drawn.

2. Experimental apparatus

The three devices used in the experiments are the large HP and MICP sources and the compact HP source. The large HP consists of a 14 cm diameter, 23 cm long quartz chamber attached to a stainless tube (see figure 1(*a*) and [20, 28]). The source is excited at 13.56 MHz by a double-turn $m = 0$ antenna positioned 6 cm from the metal end plate. Two magnetic coils, the left and right ones with separately controlled currents (I_{left} and I_{right}, respectively) can create

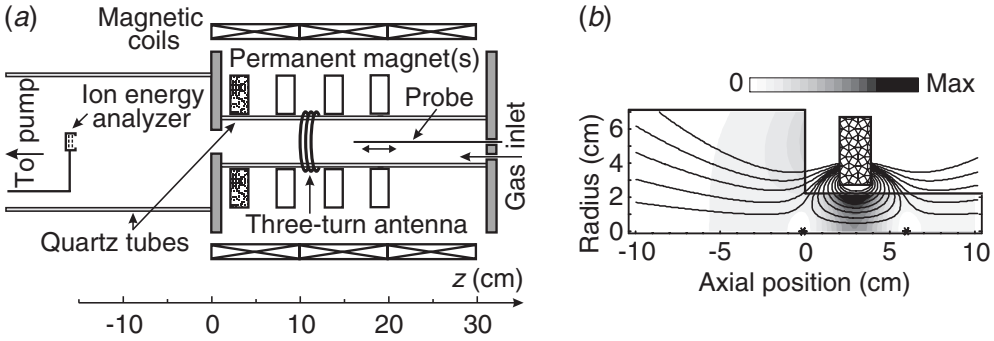

Figure 2. (*a*) Schematic view of the compact HP source. (*b*) Magnetic lines and constant $|B|$ contours for the annular PM; stars show the null points on the axis.

both the uniform and nonuniform magnetic fields. Measurements were performed with the use of electric and magnetic probes and the dipole antenna.

The MICP source consists of a 20 cm diameter, 30 cm long stainless chamber limited by the metal substrate table and the quartz window (figure 1(*b*)). The discharge is excited by a single-turn $m = 0$ antenna located above the window and powered from a 13.56 MHz generator. Three coils, the upper, medium and lower ones (the latter is situated 12 cm under the table and is not shown in figure 1(*b*)) with separately controlled currents ($I_{\rm up}$, $I_{\rm mid}$ and $I_{\rm low}$, respectively) could create the magnetic field of variable configuration. Measurements were performed with radially movable electric and magnetic probes.

A compact HP source consists of a 4.5 cm diameter, 32 cm long quartz discharge chamber attached to a 14 cm diameter quartz drift chamber (figure 2(*a*)). The discharge was excited at 13.56 MHz by a three- or four-turn $m = 0$ antenna. The basic magnetic field was created by annular PMs made of barium ferrites magnetized along the axis; however, in the present experiment only the leftmost PM was installed. The magnetic field of the PM is strongly nonuniform, with null points (cusps) near the ends (figure 2(*b*)). To vary the magnetic configuration, we used the electromagnet (EM) with separate current control in three sections. Plasma parameters were measured by an axially movable probe.

3. Enhanced operating modes

Large HP. Strong increase of the plasma production and concomitant wave effects in the large HP with the nonuniform magnetic field were recently examined in detail [20] and the results are summarized here. Axial density profiles are shown in figure 3(*a*) for the uniform (both coils in figure 1(*a*) are equally powered producing 70 G) and nonuniform ($I_{\rm left} = 0$) fields. As the axial particle loss is dominant, plasma confinement worsens in the nonuniform case. So, the effect of density increase apparently results from alterations of the wave characteristics. Indeed, in the uniform case the rf B_z field is radially large scale and relates to the helicon wave. In the nonuniform case, a small-scale wave structure is found to propagate from the antenna along the magnetic lines, as shown in the inset of figure 3(*a*). This structure is attributed to the transitional waves (between helicons and electrostatic waves) with perpendicular wave numbers $k_\perp \approx \delta^{-1}$, where $\delta = c/\omega_{\rm pe}$ is the collisionless skin size. Theory predicts that in the uniform case the absorption occurs mainly at the plasma periphery due to the surface mode conversion of the helicons into electrostatic waves [36]. In the nonuniform case, the surface mode conversion under the antenna is depressed if the inclination of magnetic lines to

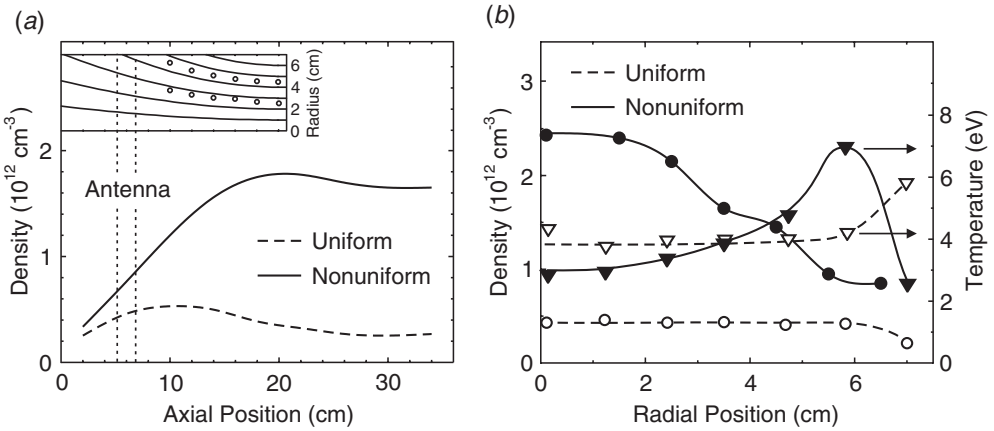

Figure 3. (*a*) Plasma density on the axis of the large HP, for the uniform and nonuniform magnetic field. The inset shows the magnetic lines in the nonuniform case and trajectories of the small-scale peaks of the rf B_z field. (*b*) Radial profiles of the plasma density and electron temperature in the uniform and nonuniform fields, at $z = 18$ cm.

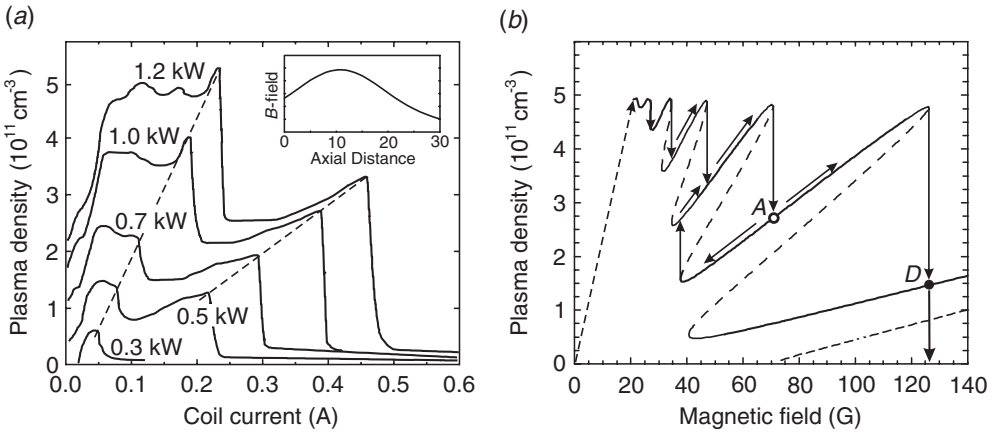

Figure 4. (*a*) Plasma density measured in the MICP by the lower probe versus upper coil current, I_{up}, at various input powers and $I_{mid} = I_{low} = 0$. The maximum magnetic field is 360 G A^{-1} and $p_{Ar} = 5$ mTorr. (*b*) Variation of the plasma density with the magnetic field predicted from the power balance consideration. Arrows around point *A* demonstrate hysteresis of the density variation; the discharge disruption is predicted at point *D*.

the plasma surface exceeds the critical angle $\theta \approx \omega/\omega_{ce}$ where ω and ω_{ce} are the driving and cyclotron frequencies, respectively. As a result, the helicons penetrate deeper into the plasma and deposit the power closer to the centre. Together with the high electron conductivity along the magnetic lines, this effect is thought to enhance the plasma production. One can see in figure 3(*b*) the hot electron layer that extends from the antenna along the magnetic lines and is a principal factor in the ionization.

Magnetized ICP. The MICP is even more sensitive to the magnetic configuration. The plasma density as a function of B produced by only the upper coil (figure 4(*a*)) first grows sharply and then varies with multiple jumps until a discharge disruption occurs at a critical field.

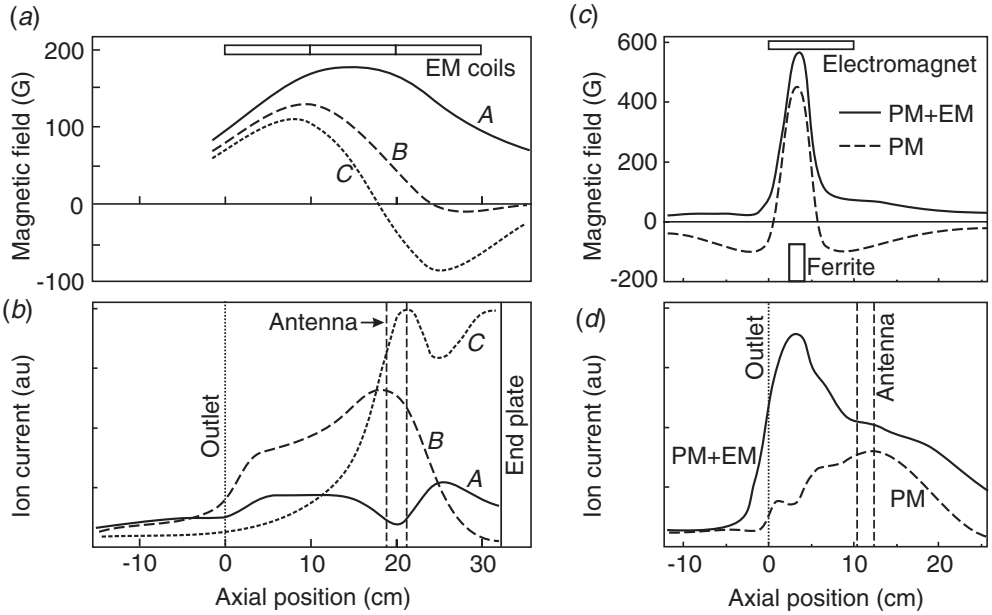

Figure 5. (*a*) Magnetic field of the EMs and (*b*) respective profiles of the ion saturation current along the axis of the compact HP, at various currents in the right EM section. (*c*) Magnetic field with the EM turned off (PM) and turned on (PM + EM), and (*d*) respective profiles of the ion saturation current on the axis.

The density grows twice if all the three coils are engaged to produce B converging from the antenna along the whole device (see figure 7(*a*)). The radial density profile is centrally peaked in the high density mode that arises at lower B as a 'blue mode' with a bright core. Theory predicts the density jumps to originate from sharp resonances of the wave eigenmodes that are combined by the helicons and evanescent surface waves localized at the plasma–quartz interface. Computed plasma loading resistance as a function of density is smooth at low B, but at $B > 20$ G it acquires high and narrow peaks corresponding to the eigenmodes with axial wavelengths $\lambda \approx 4L/(2p+1)$ where L is the device length and p an integer. So, the source with the metal chamber is a high-Q resonator for the waves. The reason is that the mode conversion of the helicons into electrostatic waves, which occurs in the HP mainly near the nonconducting chamber walls and results in strong helicon damping, is depressed in the MICP. The density variation theoretically predicted from the power balance (figure 4(*b*)) satisfactorily correlates with the experimental behaviour.

Compact HP. Effects of the magnetic configuration are especially important in the compact source with the PM (figure 2(*a*)) because strong field nonuniformity with the null points (cusps) can impede the wave propagation and plasma flow. To find an optimal configuration, we tried the PM and EM in various combinations. At first, the PM was removed and only the EM was used to verify that the effect of enhanced plasma production is inherent to the compact HP as well as to the large HP. Figure 5(*a*) shows magnetic profiles for equal currents in all the EM coils (curve A) and for two opposite currents in the right section (curves B and C) chosen so as to provide the field cusp on the right or left from the antenna. As seen from the respective profiles of the ion current in figure 5(*b*), the plasma production is directional and enhanced if the antenna is placed in a weaker field (cases B and C).

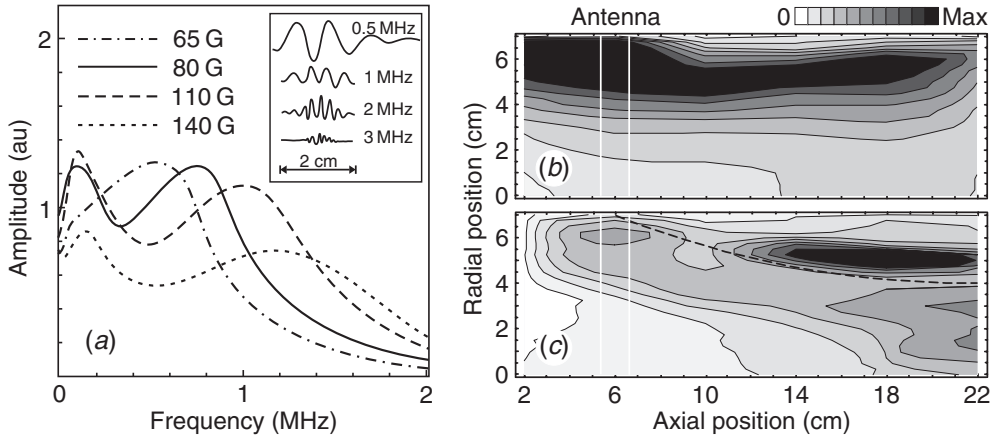

Figure 6. (*a*) Envelopes of the low-frequency spectra in the large HP, for uniform B and $p_{\mathrm{Ar}} = 5$ mTorr. The inset shows correlation functions, at $B = 80$ G. (*b*) Measured spatial distribution of the oscillations at 300 kHz, for uniform B. (*c*) The same for nonuniform B, with the dashed curve indicating the magnetic line.

The discharge burns into the stronger field and can be switched from the left to the right by displacing the cusp relative to the antenna. Next, the PM was installed and used either alone or in combination with the left EM section, to eliminate the cusp (figure 5(*c*)). The respective profiles in figure 5(*d*) show that the ion current peaks under the antenna and little plasma escapes the source with the PM alone. With the EM engaged, the plasma density increases and peaks under the PM, resulting in much better plasma ejection from the source. Though detailed measurements were not conducted, the effect of magnetic configuration in the compact HP is so similar to that in the large HP that its physical origin is thought to be the same.

4. Nonlinear wave phenomena

Low-frequency turbulence in the large HP. Our recent experiments with the $m = 1$ HP have revealed ion acoustic (IA) turbulence whose spectrum falls with frequency and has a half-width about 1 MHz [28]. The spectrum of turbulence in the $m = 0$ HP has the same width but a different shape. In the uniform field, a wide peak occurs around the lower hybrid frequency. A narrow peak, independent of B, occurs at 150 kHz (figure 6(*a*)). Oscillations show quite long azimuthal correlation at any frequency (see the inset in figure 6(*a*)), but a short radial correlation. The waves propagate along the electron gyration with phase velocities somewhat above the IA velocity, which can result from oblique propagation relative to the line between the probe tips, and/or from parametric increase of the frequency. Turbulence has comparable intensities in the uniform and nonuniform B cases but different spatial distributions. In the uniform B case, the intensity is maximal under the antenna and has a long peripheral peak parallel to the wall (figure 6(*b*)). In the nonuniform B case (figure 6(*c*)), the distribution is aligned with the magnetic lines and has a slight peak under the antenna and a stronger downstream peak around the location of the small-scale wave structure at the fundamental frequency (cf the inset in figure 3(*a*)). The amplitude of turbulence pulsations estimated from the noisiness of the ion saturation current is $\delta n/n \approx 0.05$; i.e. twice less than when $m = 1$ HP [28].

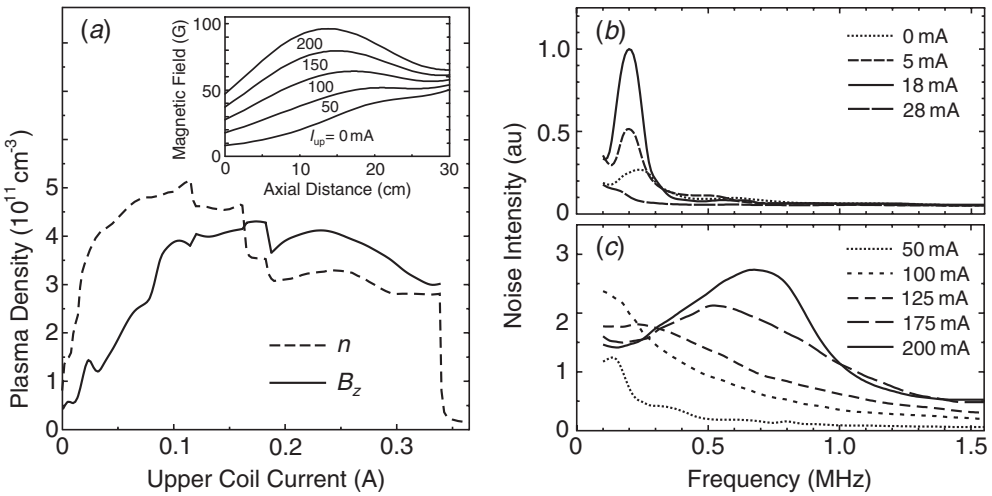

Figure 7. (*a*) Plasma density and the rf B_z-field as functions of I_{up} in the MICP, at $z = 25$ cm and $r = 6$ cm. $I_{mid} = 2$ A, $I_{low} = 0.3$ A, $P_{RF} = 750$ W and $p_{Ar} = 3.8$ mTorr. The inset shows the magnetic profiles on the axis, at various I_{up}. (*b*) and (*c*) Envelopes of the low-frequency spectra measured at the same location, for various I_{up}.

Low-frequency turbulence in the MICP. Variation of the plasma density with the upper coil current I_{up} (see figure 1(*b*)) and the low-frequency spectra at various I_{up} were measured at the same position in the MICP by the lower probe (figure 7). One can see two different regimes of the excitation of low-frequency oscillations. At low I_{up}, the spectrum is narrow and has a 200 kHz peak that first grows with I_{up} but then disappears (at $I_{up} \approx 30$ mA). In this regime, oscillations show quite good azimuthal correlation and phase velocities 1.5–2 times exceeding the IA velocity. At higher I_{up}, a wide-band spectrum arises; it broadens out with growing I_{up} and includes a wide peak moving to higher frequencies. Oscillations in this regime are much more intense and short-correlated. As the appearance of the wide-band spectrum correlates with the sharp increase of the rf field at the same position (figure 7(*a*)), it can be attributed to a parametric instability.

Field enhancement and ponderomotive effect near the metal surfaces. Intense nonlinear effects in the ICMPs are expected in the edge layer in front of metal surfaces transverse to the magnetic lines. Figure 8(*a*) shows the rf E_z field measured by the dipole antenna along the axis of the large HP, under uniform B. The field tends to grow rapidly towards the metal end plate ($z = 0$). The value of 4 V cm^{-1} measured in the final available point is already strong enough: the electron oscillatory velocity $v_z = eE_z/m_e\omega \sim v_{te}$, the thermal velocity.

The E_z field in the $m = 0$ plasma is maximal near the axis where it can be expressed as $E_z \approx F_z(z)J_0(k_\perp r)\exp(-i\omega t)$ with J_0 being the Bessel function and $k_\perp$ an effective perpendicular wave number. Considering that $B_\theta \approx H_\theta(z)J_1(k_\perp r)\exp(-i\omega t)$, one derives from Maxwell equations $F_z = -iN_\perp(\omega/\omega_{pe})^2 H_\theta$ ($N_\perp$: the transverse refractive index). If the width of the edge layer $\Delta z < \delta(\omega_{ce}/\omega)^{1/2}$ where $\delta = c/\omega_{pe}$, $H_\theta \approx$ const within the layer and, therefore, $F_z \sim n^{-1}$, which is a simple consequence of the j_z current continuity. Computed profile of E_z fits well with the measured one (figure 8(*a*)). (Note that the field enhancement is also expected near the metal bottom plate of the MICP.) In strong E_z field the electron motion becomes quasi-one-dimensional. If the rf electron excursion is less than Δz, the nonlinear

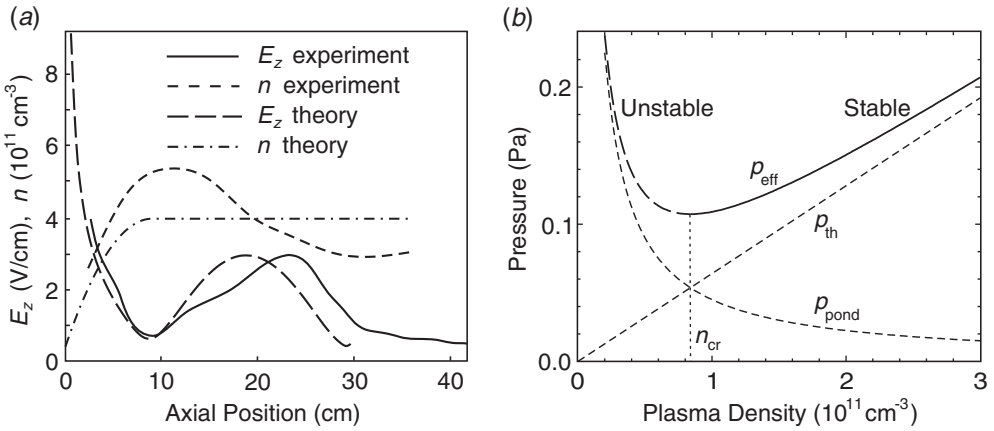

Figure 8. (*a*) Axial profiles of the rf E_z field on the axis measured by a dipole antenna and computed for the nonuniform density profile with edge-to-bulk density ratio 0.1. (*b*) Thermal, ponderomotive and effective pressures versus plasma density, at $T_e = 4$ eV. Ponderomotive pressure was computed for the helicon mode with perpendicular wave number $k_\perp = 1$ cm^{-1} and rf magnetic field $H_\theta = 1$ G.

force acting on the electron is reduced to the adiabatic ponderomotive force, $f_{\rm pond} \sim F_z^2 \sim n^{-2}$. In the averaged momentum equation, this force can be combined with the thermal pressure to yield the effective pressure which is shown as a function of density in figure 8(*b*). Below a critical density the plasma is unstable, $\partial p_{\rm eff}/\partial n < 0$; i.e. any density drop increases the pressure which gives rise to further plasma extrusion and concomitant field enhancement. So, the edge layer with $n < n_{\rm cr}$ can undergo the nonlinear instability whose saturation is expected under violation of the adiabatic condition and/or owing to phenomena like stochastic electron heating, parametric instabilities, etc.

5. Conclusions

Magnetic field configuration is a powerful means for maximization, at a fixed input power, of the plasma output in the ICMPs. The effect results from alterations in the wave performance rather than in particle confinement. In the HP, the plasma density grows from the antenna into the converging field, which was argued to result from propagation characteristics of the helicons and peculiarities of their mode conversion in plasma with the density gradient non-perpendicular to the magnetic lines. In the MICP, the plasma density is maximal at lower magnetic fields, increases in converging magnetic field and varies with jumps at increasing B, which are thought to arise from alternation of the cavity eigenmodes. Substantial growth of the plasma outflow in the compact HP with the PM was attained by eliminating the field cusps with the use of the EM. Favourable magnetic configuration may hopefully be reproduced using only PMs.

Ion acoustic turbulence in the megahertz range was detected in both the HP and the MICP. Its spectrum broadens with increasing magnetic field and spatial distribution depends strongly on the magnetic configuration. In the HP with nonuniform field, the peak of turbulence intensity correlates with the density peak; however, the role of turbulence in the discharge performance is not yet clear. Axial rf electric field in the HP demonstrates a strong increase towards the metal end plate. This is expected to drive various nonlinear and stochastic processes and to influence the edge plasma stability.

Acknowledgments

One of the authors (KPS) acknowledges with thanks the support of his trip to the 12th ICPP (Nice, France, 25–29 October 2004) by the Science and Technology Center in Ukraine and by the ICPP LOC. This work was partly supported by the State Fund for Basic Research under contract F7/253-2001.

References

[1] Boswell R W and Chen F F 1997 *IEEE Trans. Plasma Sci.* **25** 1229
[2] Chen F F and Boswell R W 1997 *IEEE Trans. Plasma Sci.* **25** 1245
[3] Stevens J E, Sowa M J and Cecchi J L 1995 *J. Vac. Sci. Technol.* A **13** 2476
[4] Shinohara S, Takechi S and Kawai Y 1996 *Japan. J. Appl. Phys*. **35** 4503
[5] Godyak V A and Alexandrovich B M 2004 *Phys. Plasmas* **11** 3553
[6] Tynan G R *et al* 1997 *J. Vac. Sci. Technol.* A **15** 2885
[7] Lee H J, Yang I D and Whang K W 1996 *Plasma Sources Sci. Technol.* **5** 383
[8] Chang Díaz F R 1999 *Trans. Fusion Technol.* **35** 87
[9] Miller R L *et al* 2001 *Bull. Am. Phys. Soc.* **46** 132
[10] Scime E E *et al* 1998 *Plasma Sources Sci. Technol.* **7** 186
[11] Shamrai K P *et al* 1997 *J. Physique Coll.* IV **7** C4-365
[12] Hong I S *et al* 2000 *Rev. Sci. Instrum.* **71** 1385
[13] Sasaki K, Kokubu H, Hayashi D and Kadota K 2001 *Thin Solid Films* **386** 243
[14] Miroshnichenko V I *et al* 2003 *Nucl. Instrum. Methods* B **201** 630
[15] Light M and Chen F F 1995 *Phys. Plasmas* **2** 1084
[16] Shinohara S, Miyauchi Y and Kawai Y 1995 *Plasma Phys. Control. Fusion* **37** 1015
[17] Krämer M 1999 *Phys. Plasmas* **6** 1052
[18] Chevalier G and Chen F F 1993 *J. Vac. Sci. Technol.* A **11** 1165
[19] Braginskii O V, Vasil'eva A N and Kovalev A S 2001 *Plasma Phys. Rep.* **27** 699
[20] Virko V F, Shamrai K P, Kirichenko G S and Virko Yu V 2004 *Phys. Plasmas* **11** 3888
[21] Godyak V 2003 *Plasma Phys. Control. Fusion* **45** A399
[22] Stenzel R L 1991 *Phys. Fluids* B **3** 2568
[23] Porkolab M, Arunasalam V and Ellis R A 1972 *Phys. Rev. Lett.* **29** 1438
[24] Boswell R W and Giles M J 1976 *Phys. Rev. Lett.* **36** 1142
[25] Kaganskaya N M, Krämer M and Selenin V L 2001 *Phys. Plasmas* **8** 4694
[26] Kline J L *et al* 2002 *Phys. Rev. Lett.* **88** 195002
[27] Kline J L and Scime E E 2003 *Phys. Plasmas* **10** 135
[28] Virko V F, Kirichenko G S and Shamrai K P 2003 *Plasma Sources Sci. Technol.* **12** 217
[29] Corr C S *et al* 2004 *Phys. Plasmas* **11** 4596
[30] Boswell R W *et al Phys. Plasmas* **11** 5125
[31] Akhiezer A I, Mikhailenko V S and Stepanov K N 1998 *Phys. Lett.* A **245** 117
[32] Mikhailenko V S, Stepanov K N and Scime E E 2003 *Phys. Plasmas* **10** 2247
[33] Light M, Chen F F and Colestock P L 2001 *Phys. Plasmas* **8** 4675
[34] Brown R D, Gilland J H, Hershkowitz N and Breun R A 1995 *J. Vac. Sci. Technol.* A **13** 865
[35] Lho T *et al* 1998 *Phys. Plasmas* **5** 3135
[36] Virko V F, Kirichenko G S and Shamrai K P 2002 *Plasma Sources Sci. Technol.* **11** 10